

## Evaluation of Carbonate Platform in the Deep-water Dangerous Grounds, NW Sabah Platform Region, Malaysia

Atanu Banerjee, Ahmed Mohamed Ahmed Salim, Maman Hermana Husen, Abdul Halim Abdul Latiff

Centre for Subsurface Imaging, Department of Geosciences, Universiti Teknologi PETRONAS, 32610, Seri Iskandar, Perak, Malaysia

Received October 29, 2021, Accepted March 17, 2022

### Abstract

During past decades, worldwide deep-water hydrocarbon exploration has attained interest with significant commercial discoveries. The upside exploration possibilities of worldwide deep-water basins are not explored to their full potential, and it has been expected that near future, many new discoveries will come. Globally, deep-water petroleum settings of different basins are highly variable. Effective exploration exertions in the frontier region will hang on to the application of knowledge gathered from an improved understanding of the well-explored basins with known petroleum systems. In Southeast Asia, a proven petroleum system exists in the Sabah basin and has a substantial financial influence on this region. Present-day hydrocarbon discovery in the deep-water region, NW Sabah Trough encouraged an inclusive inquiry of the adjacent territory, e.g., the hydrocarbon prospectivity in the Dangerous Grounds region, where the exploration activities are in the initial phase. Earlier, the analysis was principally intensive on infrequent 2D seismic data and gravity-magnetic data investigation. An organised way of the seismic attribute analysis and well log interpretation of the carbonate platform of Late Oligocene- Middle Miocene age has not been conferred thus far in the published literature. In this research work, newly obtained 3D seismic data with high-resolution and well information have been used to evaluate the carbonate platform. Seismic sections reflect the faults related to syn-rift tectonic activity that was also prominent in the post-rift section. The variance extraction map reveals the structural trend in the platform region and also the growth of the reef on top of the carbonate platform. RMS amplitude extraction map reflects the delivery of carbonate platform with higher amplitude value; sweetness extraction map reveals the fault-related lateral discontinuities. Significant evidence of facies changes, carbonate to clay/shale has been observed. Density vs gamma-ray and density vs neutron porosity cross plot reflect the presence of limestone, sand, shaly sand/siltstone, and carbonaceous shale. Vp vs Vs cross plot reflects a linear trend. Vp/Vs vs P-impedance cross plot depicts the reservoir rock carbonates that are water-bearing. Mu-rho vs density cross plot discriminates the lithologies as carbonate, shaly sand/siltstone, shale. During the Middle Miocene end, the high influx of siliciclastic sediments has been observed, resulting in the demise and burial of carbonate.

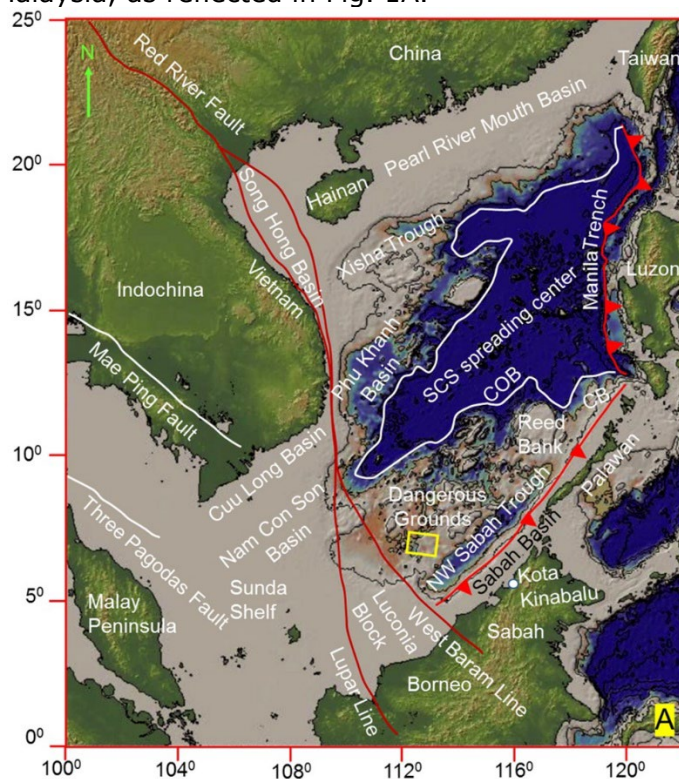
**Keywords:** Carbonate platform; Cross plots; Dangerous Grounds; Sabah basin; Vp/ Vs vs P-Impedance.

### 1. Introduction

The South China Sea (SCS) basins have witnessed the prolific growth of Late Oligocene-Middle Miocene carbonate as suggested by previous workers like Ding *et al.*, [1]; Franke *et al.*, [2]. Recent studies in the Dangerous Grounds and Reed Bank area by several workers have brought out the widespread Oligocene-Miocene carbonate [1,3-5], Nido carbonate platform of Oligocene-Miocene age at West Palawan Basin, Zhujiang Formation of Miocene age from Pearl River Moth Basin, Xisha carbonate of Miocene age, Miocene carbonate platform from Triton and Phan Rang, Vietnam and Central Luconia carbonate, Sarawak [6-7]. There are various parameters like tectonic lineaments, basement structures, paleo-oceanography, sea-level

changes, a clastic influx that can control the carbonate growth, morphology, and distribution as suggested by Yubo *et al.*, Shao *et al.*, Wilson, and Qing Sun and Esteban [8-11].

In Sarawak Basin, the Miocene carbonates of Central Luconia is already a proven hydrocarbon territory in Malaysia, where 40% of the gas reserves come from the Miocene carbonate of offshore Sarawak. Over 200 carbonate bodies have been seismically analysed [12]. Till now, hydrocarbon exploration is mainly restricted to the nearshore carbonates or the shelf break carbonates of the continental shelf region in SCS. There are not many isolated carbonate platforms have been examined, and many new discoveries have been made [6-7,13]. In 2018, deep-water hydrocarbon discovery in the carbonate of Oligocene-Miocene age by Total in well Tepat-1 in the NW Sabah Trough had established the exploration potential in this province [14]. This scientific research work has been carried out in the deep-water Dangerous Grounds area, Malaysia, as reflected in Fig. 1A.



In this part of the Dangerous Grounds, bathymetry ranges from 1000 to 2000 m. In the deep-water Sabah, Sarawak Basin, major oil companies have started exploring prospective Oligocene-Miocene carbonate plays; comparable investigations are absent in the Dangerous Grounds. Consequently, a detailed geological study has been accomplished, depending on 3D seismic and well information with improved subsurface imaging efficiency is essential to diminish the uncertainty of exploration activity in the study area.

Fig. 1.(A) The South China Sea topographic map is reflecting the basins and the major structural trends (modified after Li *et al.* [41]). The COB (Continent-Ocean Boundary) has been shown by the solid white line, as suggested by Briais *et al.* [42] on seafloor spreading anomalies. The yellow box demarcates the study area. CB represents the Calamian Block, NW-Northwest.

All former investigations have been done in this region, based on the gravity-magnetic data analysis, different vintages sparse 2D seismic interpretation and dredge sample evaluation, as mentioned in Table 1. In this research work, an organised investigation of the carbonate platform has been accomplished with the help of seismic attributes and well information. The intent of this research is to appraise the Late Oligocene-Middle Miocene carbonate platform with the help of seismic attributes and well log analysis.

## 2. Geological settings

The geological history of Malaysian basins is complex as it is situated adjacent to the actively moving plates of SE Asia. The Dangerous Grounds evolution history is linked with the provincial tectonics of the region, including the Sabah Basin tectonic history. Previously, the Sabah basin has been described as a fore-arc basin [15-16]. Later, Madon *et al.*, and Milsom *et al.*, [7,17] recommended the basin evolution as a foreland basin depending on the explanation of gravity-magnetic, seismic, burial history analysis, and drilled well information. Madon *et al.* [18] recommended that the end of seafloor spreading of the SCS has been characterised by the collisional event associated with the Sabah orogeny. The Paleogene West Crocker formation

is therefore recognised as the 'acoustic basement' to the Sabah Shelfal Basin. However, no evidence of crystalline basement has been described in the offshore province of the basin. Jong *et al.* [19] suggested that during the Miocene age, the basin observed voluminous clastic sediment deposition as an outcome of upliftment and Sabah land massif speedy erosion under supportive climatic settings. These events resulted in the progradation of NW deltas in regressive circumstances.

Table 1. Previous studies in and around the Dangerous Grounds area, NW Sabah Platform Region revealed dredge sample analysis, gravity-magnetic analysis, and 2D seismic interpretation

Type of study	Authors, years	Remarks
Dredge sample analysis	Kudrass <i>et al.</i> [21]	Dredging of Mesozoic and Cenozoic rocks from Reed Bank area
Dredge sample analysis and 2D seismic data analysis	Hutchinson and Vijayan [40]	Seismic and dredge sample analysis-Spratly Island
Gravity-magnetic data analysis	Milsom <i>et al.</i> [17]	Gravity anomalies study at Sabah-Palawan Region
Gravity-magnetic and 2D seismic data analysis	Vijayan <i>et al.</i> [3]	Crustal character and thickness study-Dangerous Grounds and NW Borneo Trough
2D seismic data analysis	Clift <i>et al.</i> [44]	Reflection evidence for a Dangerous Grounds minibasin
	Ding <i>et al.</i> [46]	Seismic stratigraphy and tectonic structure
	Steuer <i>et al.</i> [4]	Oligo-Miocene carbonates in Reed Bank and Palawan region
	Franke <i>et al.</i> [2]	Rifting evolution of the SCS
	Chang <i>et al.</i> [5]	Seismic sequence stratigraphy of carbonate platform-Taiping Island
	Peng <i>et al.</i> [22]	Rift to drift in the Dangerous Grounds area

The opening of the SCS has directly linked with the tectonic evolution of Dangerous Grounds. In the Dangerous Grounds region, the sedimentation of the Cenozoic age has been interrupted by unconformities as identified by the interpretation of marine seismic data by the present study and also confirmed by the studies carried out by previous workers like Hinz and Schlüter [20] and Hutchison and Vijayan [13]. Hinz and Schlüter [20] and Kudrass *et al.* [21] suggested that the Reed Bank and Dangerous Grounds are underlain by a stretched continental crust which was deltaic sediments, magmatic rocks, garnet-mica, amphibolites-metamorphic rocks of Late Triassic age, collected from the dredging of submarine outcrops. Kudrass *et al.* suggested that the oldest rock present in the Reed Bank and Dangerous Grounds region is of Late Triassic to the Jurassic age, as it was confirmed by radioactive dating-k/Ar and biostratigraphic investigation.

A recent investigation by Peng *et al.*, [22] recommended that in the Dangerous Grounds, Reed Bank, and adjoining areas during the early rifting phase, the main structures composed are large half grabens restrained by listric faults and separations, grabens linked with high angle normal faults and in the hyper-extended continental crust, significant existence of rotated fault blocks. Some places within the syn-rift sediment, Middle Eocene intrusive (Fig. 1C) and in the post-rift section, Early Miocene intrusive have been observed by Banerjee and Salim [23]. Recent studies by Franke *et al.*, and Hutchison and Vijayan [2,13] suggested that around 15 MY, the termination of SCS spreading coincides with the collision of the microcontinental blocks, which were southwards drifted, along with the Dangerous Grounds with the northern Borneo margin. The collision between the two continental blocks resulted in a major territorial uplift, erosion and was represented by MMU (Middle Miocene Unconformity), a provincial unconformity.

The depositional history of Dangerous Grounds (Fig.1B, 1C) can be described as during Paleocene-Early Oligocene age rifting took place with the siliciclastic deposition in the half grabens. Late Oligocene-Middle Miocene has evidenced the deposition of the shallow marine carbonate platform, reefs on pre-existing structurally high areas and clastic in lows. During this period, vertically stacked isolated channels, the convex-upward sand filling, meandering channel-levee complex, ox-bow lake, and point bar features are also prominent. Mass transport deposits with the prominent existence of erosional grooves have been noticed by



Banerjee *et al.*, [24]. The significant presence of slides, debris flow, turbidites has been observed above the MMU. After the MMU event, the Dangerous Grounds area has experienced the deposition of pelagic and hemipelagic sediments under passive margin conditions during Pliocene to recent age [14,23].

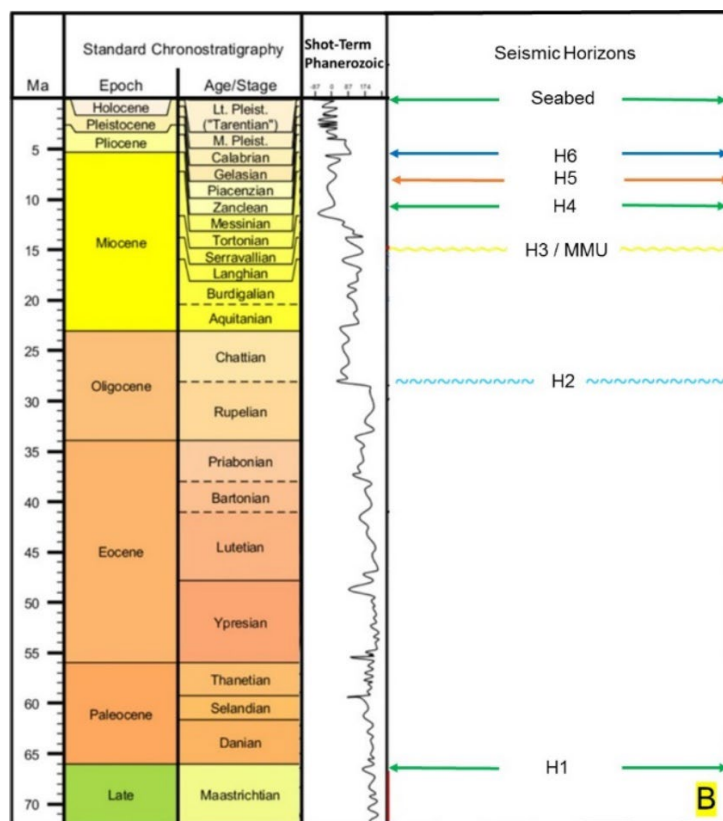


Fig. 1(B) Stratigraphic chart of Dangerous Grounds where Sea-level curve has been adopted from Haq *et al.* [43] and the Geologic time scale, is from Ogg *et al.* [44]

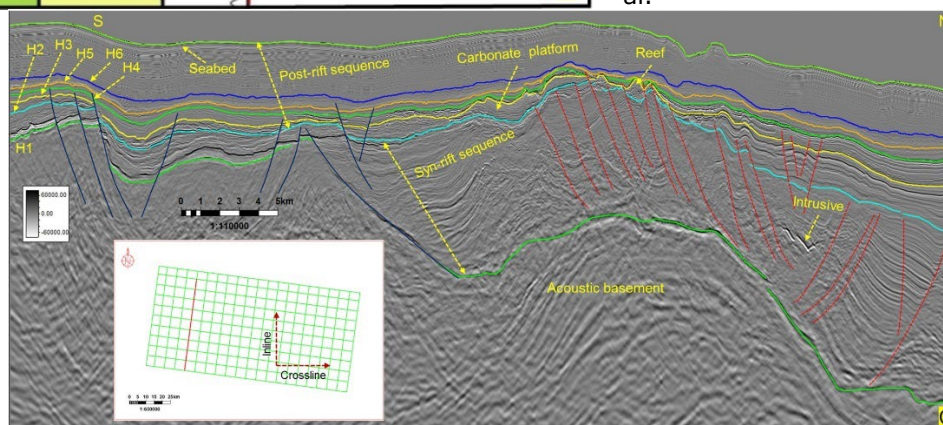


Fig 1(C) Interpreted seismic section reflecting the seismic horizons as H1- Acoustic basement top, H2-BU(Break up Unconformity), H3-MMU(Middle Miocene Unconformity), H4- Middle Miocene top, H5- Late Miocene, H6-Pliocene to recent, the sea bed (Banerjee and Salim [14]).

### 3. Materials and methods

#### 3.1. Dataset

In this present research work, the high-resolution 3D seismic Kirchhoff Anisotropic Pre-Stack Time Migration (APSTM) volume has been used. The 3D seismic data, which was acquired in 2015, covers an area of 2800 sq. km. It has a bin spacing of 12.5 X 12.5 m. This data can be used only for research purposes as it is proprietary data. In this study, drilled

wells full information are not available because of the confidentiality and sensitive nature of the data. Check shot, well completion report, selected well log curves from one well have been used for the study. Additionally, the information has been gathered from the published literature, and judiciously it has been used to excerpt maximum knowledge for seismic attributes and well log analysis of the Late Oligocene-Middle Miocene carbonate platform of the Dangerous Grounds region.

### 3.2. Methods

A synthetic seismogram has been attempted where the synthetic traces are calculated by convolving the reflection coefficient (sonic log from well-A) alongside the extracted wavelet from the 3D seismic data so that they are aligned with the corresponding event in the seismic data, as suggested by Bitrus *et al.* [25]. The seismic-well ties allow the seismic waveforms to be correlated to the stratigraphic position in the carbonate platform region. Well composite section has been prepared where lithology of the well-A has been plotted along with different log signatures.

Seismic attributes analysis has been performed to analyse the structural trend and distribution of carbonate platform in this region. In this process, variance, envelope, sweetness and amplitude extraction maps have been attempted. In view of this subsurface investigation, it has been discovered that, in comparison to the vertical dimension, depositional bodies have higher horizontal dimensions. It was suggested by Zeng [26], that taking up geologic-time surfaces from the 3D seismic data to enforce the horizontal view in seismic interpretation and to predict the depositional systems, seismic attribute map can be analysed the above-mentioned entrenched geologic time slices transversely.

In a petrophysical study, usually, a set of well logging such as density, neutron, GR, velocity and so on is essential for analysis [27]. To understand the reservoir characteristics, elastic properties (density, compressional, and shear wave) prediction and their relationship with the rock properties like lithology, porosity/ fluid content is of crucial importance [28-29]. In well log interpretation, compressional wave velocity ( $V_p$ ) data are used for lithological understanding, analysing the type of pore fluids and also the porosity. Shear waves velocity ( $V_s$ ) data are essential for mineral identification and porosity measurements [30].

In this scientific work, cross plots analysis has been carried out to understand the rock properties. To analyse the two rock properties and their attributes at the same time, cross plotting of rock properties from well log data is a very proficient way, as suggested by Buriank [31]. Omodu and Ebeniro [32] suggested that the cross-plot evaluation can be used to discriminate the reservoir. It is a visual illustration of the relationship between two or more variables to visually identify the anomalies that can be evaluated as the occurrence of hydrocarbons, other fluids, and lithologies. The major intention of this rock properties investigation is by using seismic attributes to regulate the probability of discerning among imaging architecture and reservoir facies. A typical cross plot that has been prepared in this work is the plotting of the  $V_p/V_s$  ratio versus the P-impedance.  $V_p/V_s$  ratio and P-impedance will discriminate both the fluid and lithology. This ratio reveals the fluid indication that shear waves are not responsive to fluid changes except in some specific cases of highly viscous oil, as suggested by Bello *et al.* [33] whereas compressional waves are responsive to fluid changes.

The Mu-rho method has been applied by using the square of shear wave impedance. This process will help to signify rigidity (solid component). In the present study, several cross plots have been attempted like density vs gamma-ray, density vs porosity,  $V_s$  vs  $V_p$ ,  $V_p/V_s$  vs density,  $V_p/V_s$  vs porosity,  $V_p/V_s$  vs P-impedance, Mu-rho vs density.

In this present research work, seismic attribute analysis and well log interpretation have been accomplished by utilising the Petrel software (Schlumberger).

### 4. Results

In this section, the results of well log interpretation, attribute generation, and cross plot analyses have been presented. In the study area, the main focus in the well-A is the carbonate platform section. The analysis of various logs is essential to determine the lithology and also

the study of the reservoir section. The logs that are available in well-A are gamma-ray, caliper, shallow and deep resistivity, neutron, density, P-sonic, and S-sonic. The attributes, like P-impedance and Vp Vs ratio, has been prepared from Vp, Vs, and density logs. The well data has been analysed based on lithology and fluid type (if any). Shale lithology has been defined based on its high gamma-ray value. In this well, low gamma-ray, low p-impedance values have been characterised as the presence of sand. Carbonates have been differentiated based on gamma-ray and density logs.

#### 4.1. Seismic to Well Tie

To start the seismic interpretation, seismic to well data has been calibrated. The check-shot data of Well-A has been loaded. A synthetic seismogram has been prepared (Fig. 2). In this Fig. 2, from left to right: H3/MMU is the seismic horizon (see details in the stratigraphic column at Fig. 1B), TVD(m) vs TWT(ms) correlation, Acoustic Impedance (AI)-sonic log used for reflectivity calculation, Reflection coefficient from the reflectivity series, Synthetic Seismogram generated, compared, compared against corresponding reference seismic trace from the study area. Corresponding wavelet (statistical) extracted from the seismic dataset for use. For synthetic seismogram, there are two important elements; the first one is from log data, the Acoustic Impedance derivation and also from the log data reflectivity may be derived, and the second one is the depth-related traces conversion from a depth reference to time reference so that they can be associated with the seismic section. From sonic and density logs, AI has been derived. The next step is converting the AI trace to a reflectivity trace.

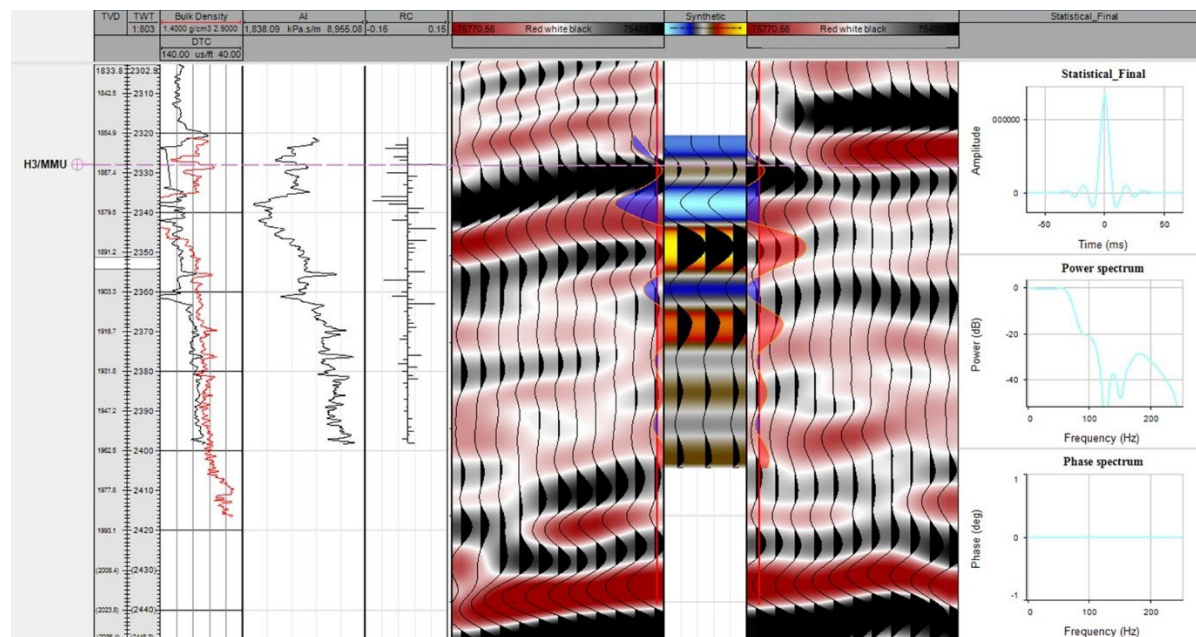


Fig. 2. Seismic to well tie and synthetic seismogram from well-A and 3D seismic data. From left to right: H3/MMU represents the seismic horizon, as it is mentioned in the stratigraphic column in Fig 1B, TVD (m) vs TWT(ms) correlation, Acoustic Impedance (AI) - sonic log used for reflectivity calculation, Reflection coefficient from the reflectivity series. From the study area, a synthetic seismogram has been prepared in comparison against the analogous reference seismic traces, corresponding wavelet(statistical) extracted from the seismic dataset for use.

#### 4.2. Seismic interpretation

The carbonate platform has been detected towards the NW part of the study area, between H2 and H4 seismic horizons, as reflected in the NE-SW seismic profile passing through wells (Fig. 3A). Their seismic component reflects high amplitude at the top, whereas internal reflection reveals moderate to lower amplitude. In the well-A section, the well has been terminated



within the carbonate section, whereas in the well-B, the well has been penetrated through the carbonate portion and terminated within the syn-rift sediments.

In the post-rift portion, syn-rift faults were active, as seen in the composite section. Pinnacle reef build-ups were noticed on the uppermost part of the carbonate platform. Their seismic characteristics reveal convergent, moderate amplitude, high-frequency reflection patterns and moderately continuous. Adjacent to the well-B section, the substantial presence of faulting has been recognised, as seen in the composite section in Fig. 3A. A prominent indication of facies change has been detected between the top and bottom of the carbonate platform, which is penetrated in the well-B. It has been expected that clay/shale was deposited in the low-lying areas (Fig. 3B).

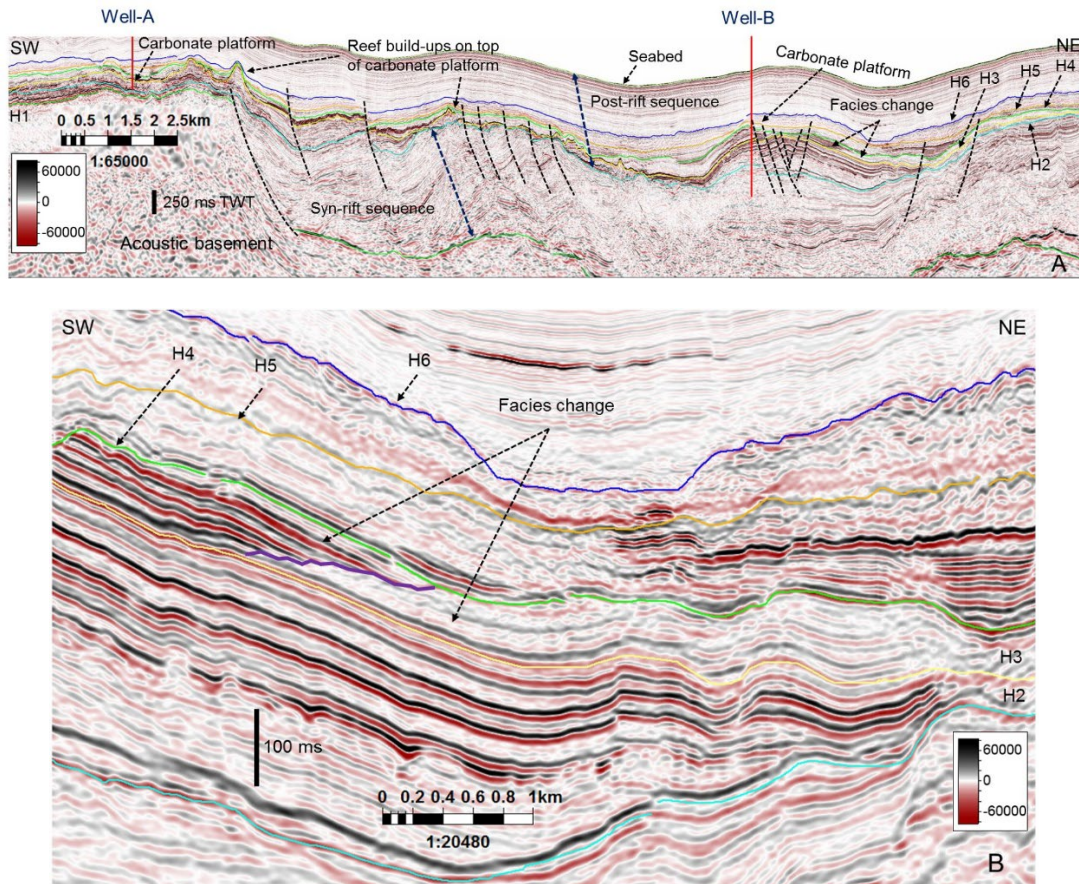
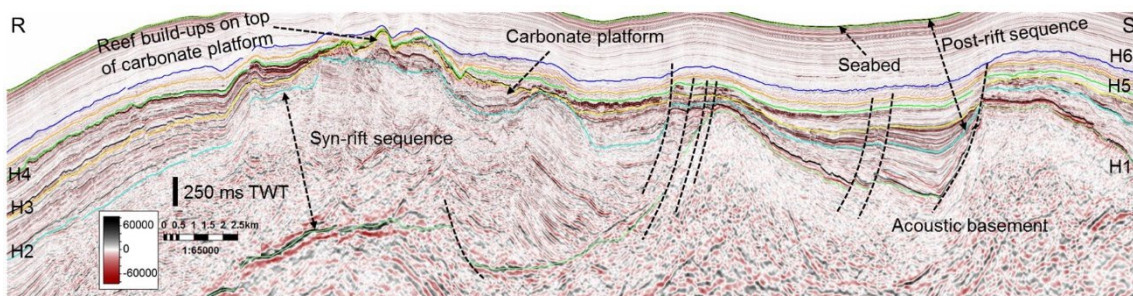
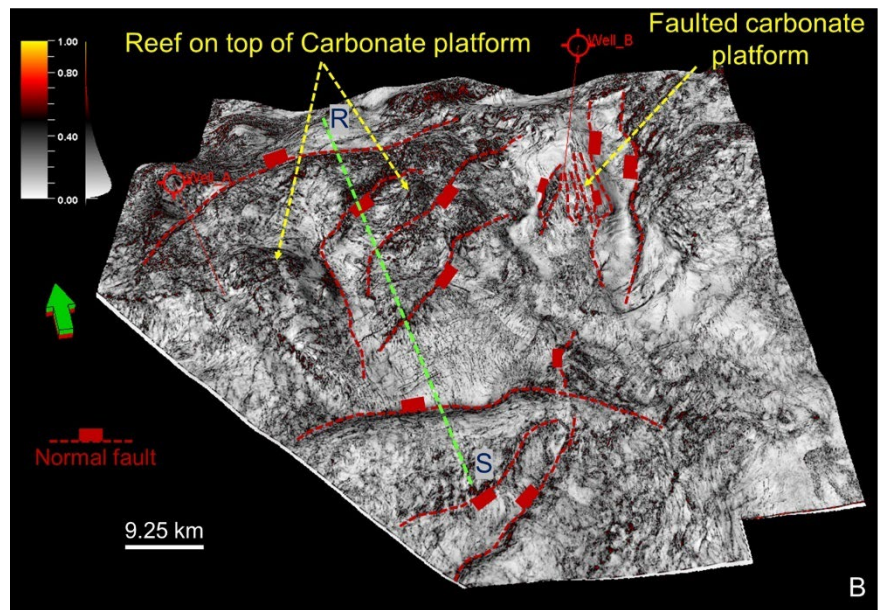
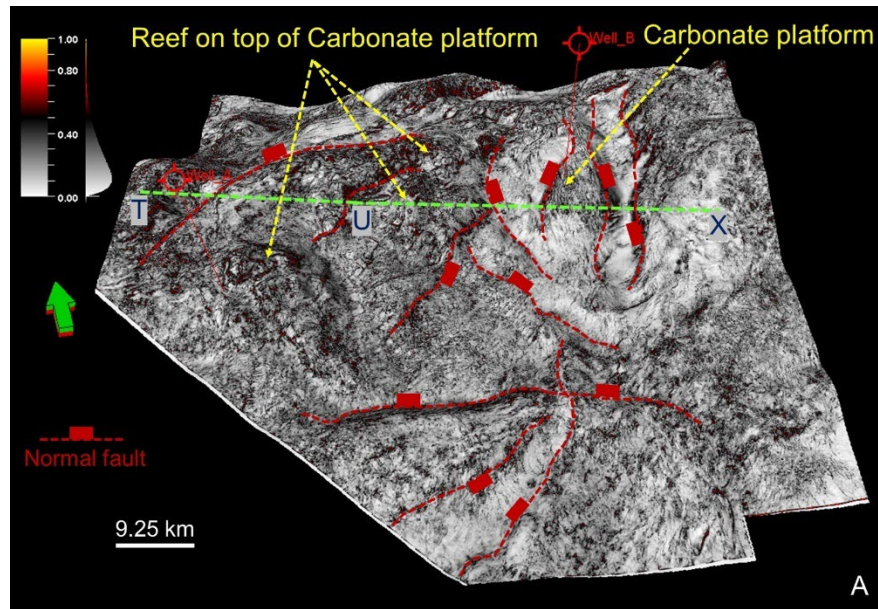


Fig. 3. (A) NE-SW composite section passing through wells reveals the presence of the carbonate platform. The carbonate platform top and base have been marked, H4 horizon as top, and H2 horizon as base. NE - Northeast, SW-Southwest. (B) Prominent occurrence of facies change is noticed near well-B. The details of the seismic horizons (H1 to the seabed) has been mentioned in the stratigraphic column in Fig. 1B.

### 4.3. Seismic attribute analysis

In this present research work, several seismic attributes have been applied to understand and characterise the internal geometry, growth pattern of the carbonate platform in this region. Two variance extraction maps have been prepared, one at the top of the Middle Miocene level and the second one 50ms below the Middle Miocene top level. Normal faults have been interpreted. The variance extraction maps clearly reveal the structural trends in this region. Prominent evidence of faulted carbonate platform has been recognised (Fig. 4A, 4B). Two composite sections, R-S and T-U-X, have revealed the internal geometry in this region with prominent reefs growth on the top carbonate platform.







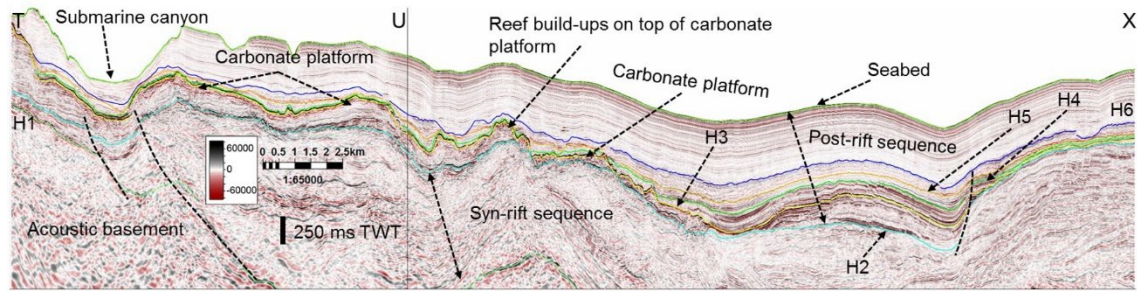


Fig. 4. Dangerous Grounds carbonate platform and the reef is exhibiting in (A) Variance extraction map at H4 horizon level, (B) The variance extraction map at 50ms below H4 horizon (vertical exaggeration ~5). NE-SW and NW-SE direction faults are prominent in the variance maps. The maps demonstrate that on the uppermost part of the structurally high region, the growth of carbonate platform and reefs are prominent. T-U-X and R-S composite sections reveal the growth of the carbonate platform within the H2 and H4 seismic markers. Reef growth is prominent on the uppermost part of the carbonate platform. The submarine canyon cut has been observed. The details of the seismic horizons are mentioned in the stratigraphic chart in Fig. 1B.

RMS amplitude extraction map has been attempted between the Middle Miocene horizon and MMU. The brighter amplitude values reveal the occurrence and distribution of the carbonate platform in the NW portion of the research area (Fig. 5A). The amplitude variation illustrates the lithology variation. The sweetness extraction map has been prepared above the MMU horizon, and it reflects the lateral discontinuities. It has been expected that these discontinuities are related to the existence of faults (Fig. 5B). Envelope extraction map has been pursued below the Middle Miocene top horizon, and it depicts the better lateral resolution and also the discrepancy in the lithology is prominent (Fig. 5C).

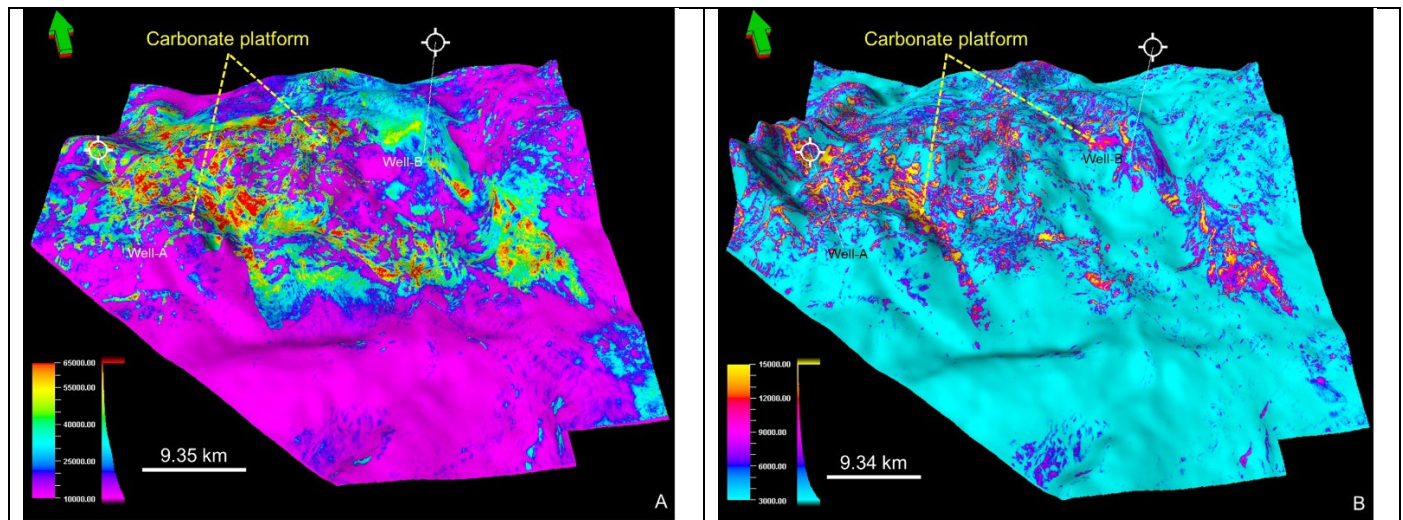


Fig. 5. (A) RMS amplitude extraction map 25ms below the H4 horizon and 25ms above the H3 horizon reveals the significant presence of the carbonate platform with a higher amplitude value. (B) Sweetness extraction map 30ms above the H3 horizon reflects the carbonate platform with a higher sweetness value.

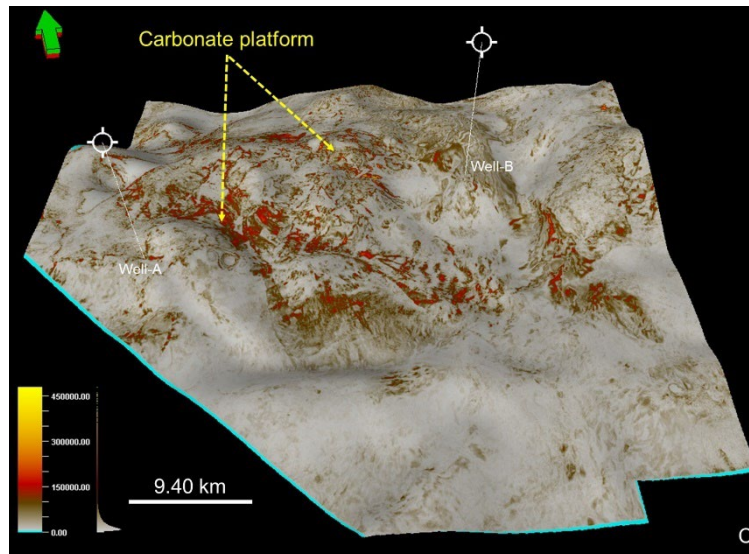


Fig 5(C) Envelope extraction map 50ms below the H4 horizon are also imitating the distribution of carbonate platform in the Dangerous Grounds region (3D map vertical exaggeration  $\sim 5$ ). H3, H4 are seismic horizons; the details of the seismic horizons are mentioned in the stratigraphic column in Fig. 1B for details)

In this present work, two-time slice maps have been attempted. The first one is at 2950ms, based on RMS amplitude, reflecting the presence of acoustic basement and the rift sediments. The orientation of the carbonate platform has been marked (Fig. 6A). The second one is the envelope attribute at 2800ms, which reveals the distribution of carbonate platform in the study area as shown in Fig. 6B.

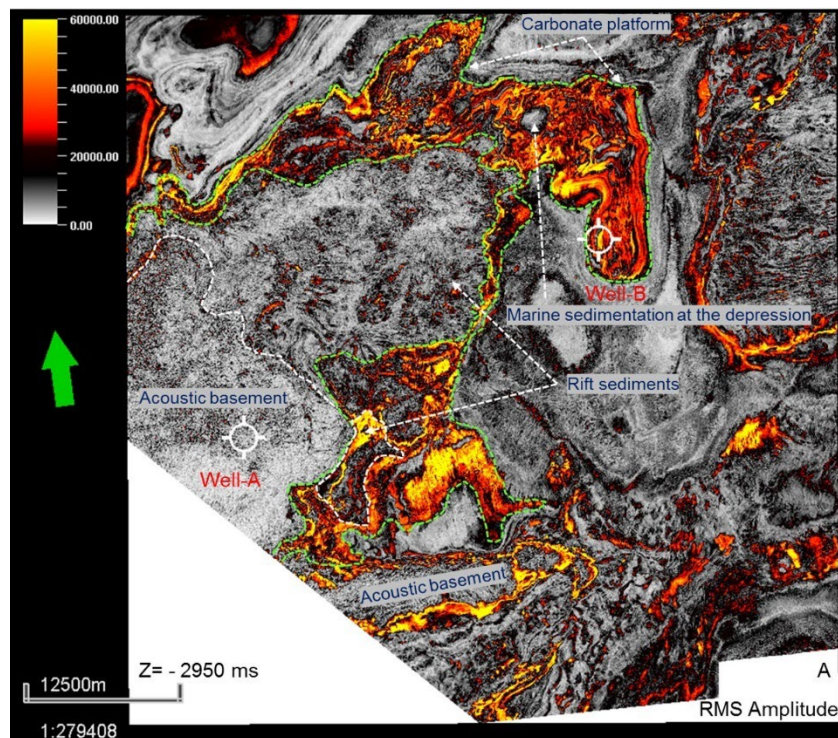


Fig. 6. (A) Time slice map of RMS amplitude ( $Z = -2950$ ms) reflecting the orientation of carbonate platform in this region. The significant presence of acoustic basement and rift sediments have been demarcated. Prominent evidence of marine sedimentation at the depression has been detected. The carbonate platform has been marked by green dotted lines.



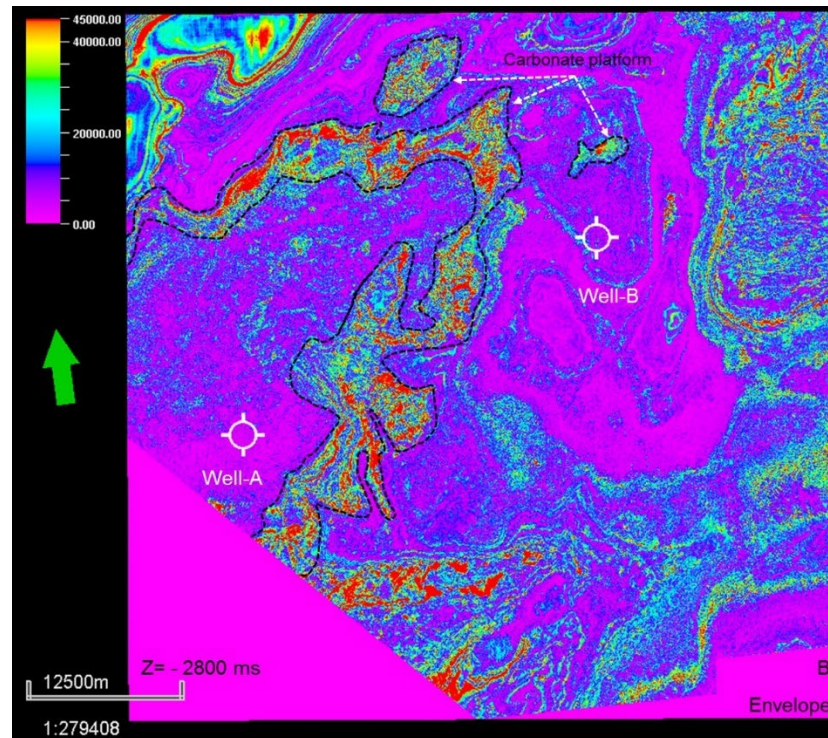


Fig 6(B) Time slice of Envelope attribute (Z= -2800ms) reveal the orientation of the carbonate platform in the research area and has been marked by black dotted lines.

#### 4.4. Well Log interpretation

Well composite section has been generated (Fig. 7) and displayed from 1886.4 to 1998m.

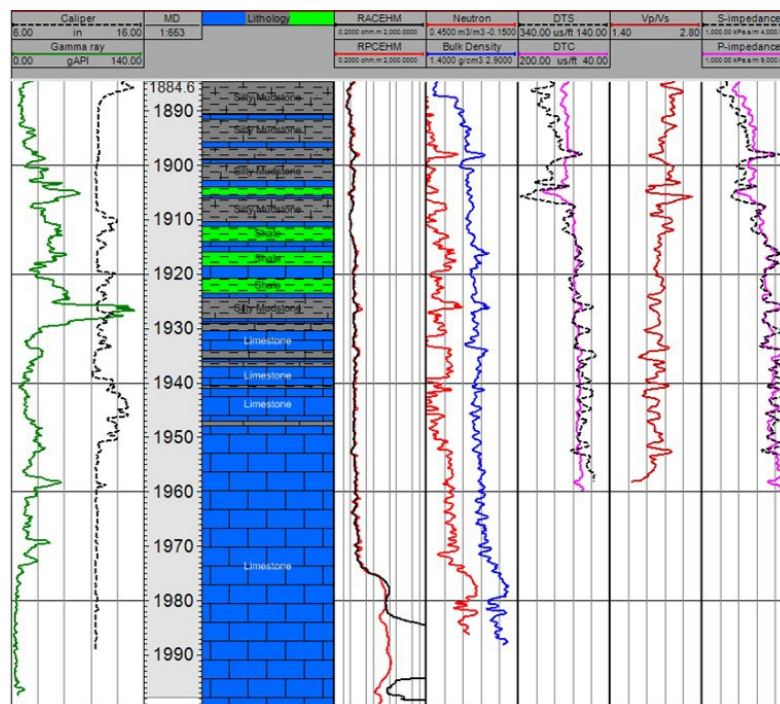


Fig. 7. Well composite section of Well-A revealed the presence of silty mudstone, shale, along with almost 60m of thick limestone.



Silty mudstone has been detected from 1886.4 to 1910m with prominent thin layers of limestone and shale; from 1910 to 1930m prominent evidence of alterations of shale, limestone, and silty mudstone have been observed. Significant evidence of limestone and thin layers of silty mudstone have been evaluated between 1930 to 1950 m. From 1950m up to the end of the well, limestone has been observed. In this section, 1909-1951m, caliper signatures suggested the hole washout; the density value is not reliable.

#### 4.5. Cross plots

Cross plot of the elastic properties based on the well data has been evaluated to understand and define the relationship between lithology and fluid properties. Several cross plots are attempted to analyse well-A.

##### Density vs Gamma-ray cross plot

The cross plot of gamma-ray against density reveals four different types of lithology based on their log responses. Limestone, sand, shaly sand /siltstone and shale have been evaluated as shown in Fig. 8A. Limestone and sand have low gamma values but higher density compared to shale.

##### Density vs Neutron porosity cross plot

Density against neutron porosity cross plot response reflects the presence of limestone, sand, shale, and carbonaceous shale at places with lower density and higher porosity value, as shown in Fig. 8B.

##### Vs vs Vp cross plot

The ratio of  $V_p/V_s$  acts as a fluid indicator because compressional waves are responsive to fluid changes, but the shear waves are not, apart from in the particular case of very viscous oil. The cross plot of shear wave velocity ( $V_s$ ) against the compressional wave velocity ( $V_p$ ) shows almost a linear trend. Evidence of transit time decreasing with depth has been observed. In the study area, the compressional wave velocity is greater than the shear wave velocity. This plot doesn't express any fluid content but reflects a linear relationship between  $V_p$  and  $V_s$ . Lithology discrimination has been carried out, as shown in Fig. 8C. There is a normal compaction effect and no high pressure in the well (mainly in the shale); drilling information also revealed the same.

##### Vp /Vs vs Neutron porosity cross plot

Cross plot  $V_p/V_s$  against neutron porosity has revealed the three different types of lithology inferred as carbonate, shale, and clean sand (Fig. 8D).  $V_p / V_s$  values between 1.8 to 2.2 and porosity range 30% to 35% indicate the presence of clean sand. In this scattered plot,  $V_p / V_s$  values for shale shows 2.0 to 2.6 with high ranges of porosity. Prominent evidence of increasing shaliness has been observed. Carbonate reflects the porosity values range between 20% to 30 %. This plot only reflects good discrimination in terms of lithology.

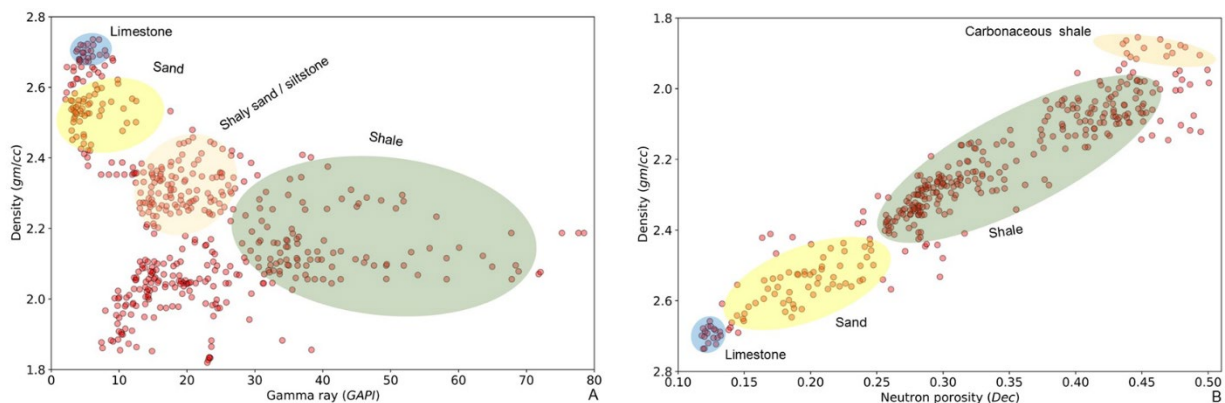


Fig.8. Cross plots of (A) Density against Gamma-ray reveal the lithological discrimination as limestone, sand, shaly sand/shale and shale. (B) Density against Neutron porosity indicates the different lithologies as limestone, sand, shale and carbonaceous shale.

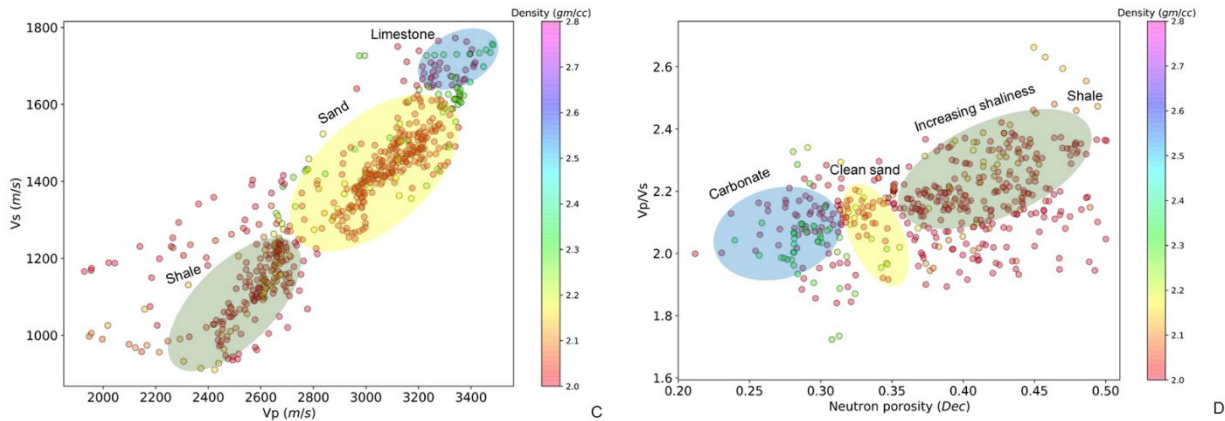


Fig.8 (C) Vs against Vp depicts three major lithologies as limestone, sand, shale. (D) Vp / Vs against Neutron porosity reflects carbonate, clean sand and shale

#### Vp / Vs vs Density cross plot

The Vp / Vs versus density cross plot (Fig. 9A) distinguishes three different types of lithology as mudstone, argillaceous mudstone, alterations of mudstone, and limestone.

#### Vp / Vs vs P-impedance

The cross plot of Vp / Vs ratio versus the acoustic impedance (P-impedance) (Fig. 9B) differentiates the well information into three zones, namely, carbonate, shale, and sand with water-bearing. This cross plot shows better lithology identification and evaluation onwards the acoustic impedance axis. Carbonate reflects the p-impedance values between 7000 to 8000 m/s\*gm/cc, shale reveals 4700-7000 m/s\*gm/cc and sand values indicates the 100% water saturation. Higher Vp / Vs value with low density and low acoustic impedance has been evaluated as silty mudstone. Vp / Vs vs. P- impedance cross plot will illustrate better fluid as well as lithology segregation which reveals that this process will better illustrate the reservoir quality in respect of lithology and fluid content than Vp vs Vs cross plot. In the present case, the reservoir rocks, including the carbonates, are water-bearing. As a result, all the carbonate's data points are clustered in one zone.

#### Mu-rho vs Density cross plot

In the Mu-rho versus density cross plot (Fig. 9C), both mu-rho and density act as lithology discriminators. Carbonate, shaly sand/siltstone, shale has been differentiated based on their characteristics. Mu-rho values are higher for sand and lower for shale. The compressibility of carbonate is less.

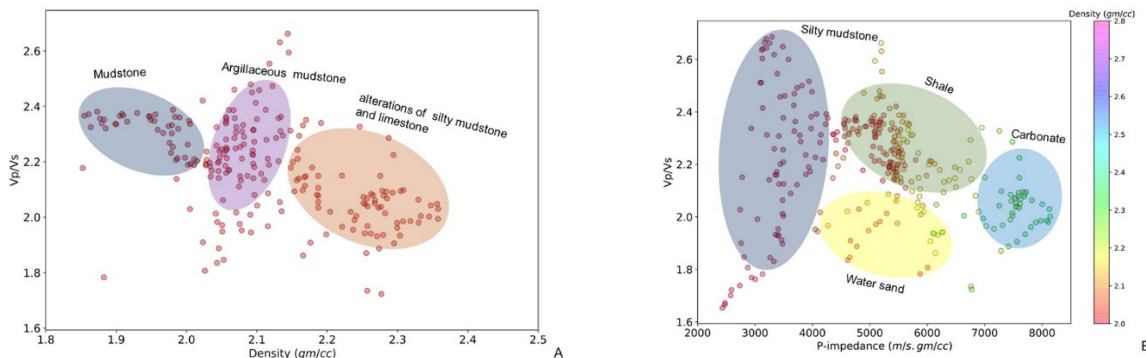


Fig. 9. Cross plots of (A) Vp / Vs versus Density reveal mudstone, argillaceous mudstone, and alterations of silty mudstone/limestone. (B) Vp / Vs versus P-impedance reflects the reservoir rock carbonate is water-bearing.

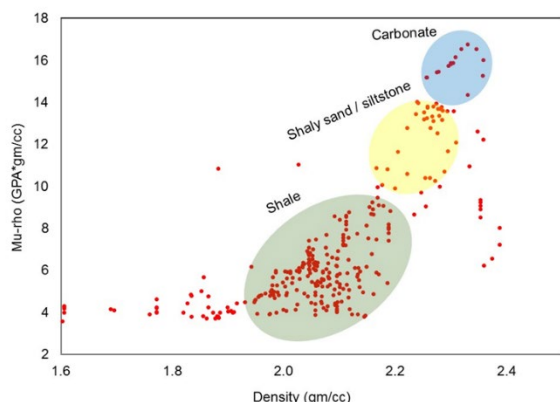


Fig. 9(C) Mu-Rho versus Density illustrates the different lithologies as carbonate, shaly sand/siltstone and shale

## 5. Discussions

In the present-day situation, exploration and production activities in the SCS region are in the expanding phase; Exploration and Production companies have started acquiring geological and geophysical data to figure out the subsurface geometry and also gathered information regarding the carbonate depositional pattern. In the Late Oligocene-Middle Miocene period, this part of the Dangerous Grounds has witnessed shallow marine platform carbonates deposition and reefs on structural highs such as volcanic seamounts and fault-bounded uplifted slabs. In the NW portion of the study area, the occurrences of the carbonate platform have been detected among H2 and H4 seismic horizons. Both the wells have been drilled on the carbonate platform, as shown in Fig. 3. Reefs were developed on the top carbonate platform, as it has been noticed in the composite sections (Fig. 3). Both the composite sections depict that rift-related faults were also effective in the post-rift section. Adjacent to the well-B, the prominent presence of faults was noticed; the variance extraction map also reveals the same. These faults may be generated after the MMU event. Near the well-B prominent occurrence of a change of facies has been noticed. Burgess *et al.* [34] recommended that in the depression, clastic sediments were commonly sheltered by gravity-induced transportation, allowing the structural highs to be free from clastic supply promoting deposition of carbonates in clear water. In the Dangerous Grounds region, the effect of the terrigenous sediment input created the obstruction for carbonate production and the carbonate growth was limited between Late Oligocene to the Middle Miocene age. Variance attribute analysis (Fig. 4) clearly reflects the fault directions of the NW part of Dangerous Grounds. The amplitude extraction map (Fig. 5A) admits a higher amplitude value and the distribution of carbonate platform in the research area. The sweetness extraction map (Fig. 5B) reveals the lateral discontinuities [35], and the envelope extraction map (Fig. 5C) reflects the better lateral resolution [36]. The time slice maps also reflected the orientation and the distribution of the carbonate platform, as shown in Fig. 6.

The well composite section reveals the thick limestone (~50m) encountered in well-A (Fig. 7). With the help of cross plot analysis, lithologies and fluid properties have been evaluated. Density and gamma-ray cross plot (Fig. 8A) reveal lithology types as limestone, sand, shaly sand/siltstone, and shale based on their responses. Based on density and neutron porosity characteristics, carbonaceous shale has been observed (Fig. 8B). Vp against Vs cross plot doesn't reflect any fluid contacts (Fig. 8C). However, the plot reflects the linear relationship between Vp and Vs [30]. Vp / Vs vs neutron porosity cross plot (Fig. 8D) demonstrates the presence of clean sand [37] with 100% water saturation and also increasing shaliness [30]. Vp/Vs vs density cross plot reveals the presence of mudstone, argillaceous mudstone, alterations of mudstone, and limestone (Fig. 9A). Vp/Vs vs P-impedance has differentiated the lithological properties, and reservoir rocks, including the carbonates, are water-bearing, as reflected in the carbonate data points in Fig. 9B. Based on the characteristics of sand as the P-impedance values ranging from 4000-6000 m/s\*gm/cc has been evaluated as water-bearing [30]. Mu-rho vs density cross plot acts as a lithology discriminator [33], prominently demarcates the presence of carbonate, shaly sand/siltstone, shale (Fig. 9C).



During the Middle Miocene end, in this region of Dangerous Grounds, rapid tectonic subsidence took place, resulting in the relative sea-level rise; at the same time, the maximum carbonate platforms were drowned as they were failed to keep pace with the speedy sea-level rise. A similar phenomenon has also been observed in the surrounding region. This drowning event during Late Miocene (10.5 Ma to 5.5 Ma) has also been reported from Xisha carbonate platforms in the NW South China Sea [38]. In the Central Luconia Region of Sarawak, the huge invasion of siliciclastic sediments and the thermal subsidence in the basin may cause the demise and burial of the carbonates, as suggested by Vahrenkamp and Hutchison [39-40].

## 6. Conclusions

The scientific work recognised broad but efficient investigation of the seismic attributes and well log analysis of the carbonate platform of Late Oligocene-Middle Miocene age from the frontier region of Dangerous Grounds, NW Sabah Platform, Malaysia. The geological settings of this area disclose a complex tectonic setting. Carbonate platform and reefs of Late Oligocene-Middle Miocene were developed on the uppermost portion of the pre-existing paleo-high section. Seismic attribute analysis reveals the structural trends in the platform region. Prominent evidence of reef growth on the uppermost part of the carbonate platform indicates the relative sea-level declination. A significant indication of facies changes from carbonate to clastic designate the paleo high region was free from a clastic supply, and the low-lying areas clastic sediments were deposited due to gravity-driven transportation. A significant indication of faults in the platform near the well-B section reflects post-MMU tectonic activity. The rock properties and attributes have been plotted to investigate the lithology and fluid content in the platform area. The density-gamma ray cross plot reveals the lithology and presence of limestone, sand, shaly sand /siltstone, and shale. Vp-Vs cross plot indicates a linear relationship, and there was no high-pressure zone in the well. Vp /Vs- porosity cross plot demarcates the presence of clean sand, whereas Vp / Vs - density plot reflects the lithology as mudstone, argillaceous mudstone. Mu-rho and density cross plot also act as prominent lithology indicators. The acoustic impedance and Vp / Vs attributes act as the most robust to distinguish the lithology and fluid properties in the carbonate reservoir zone. The research work will assist in recognising the Late Oligocene- Middle Miocene carbonate platform in this province. This may benefit to alleviate the exploration endanger in relatively unexplored areas.

## Acknowledgements

*The authors would like to express gratitude to the Centre for Subsurface Imaging (CSI) and Universiti Teknologi PETRONAS (UTP) for providing the facilities and support for this research work. Special thanks to MPM, PETRONAS, for providing data for research and approval for publication. Thanks to Schlumberger for providing the software support. This research work has been funded by YUTP Grant, Cost Centre: 015IC0-224.*

## References

- [1] Ding W, Li J, Dong C, Fang Y, Tang Y, and Fu J. Carbonate platforms in the Reed Bank area, South China Sea: Seismic characteristics, development and controlling factors. *Energy Exploration and Exploitation*, 2014; 32(1): 243–262. doi: 10.1260/0144-5987.32.1.243.
- [2] Franke D, Savva D, Pubellier M, Steuer S, Mouly B, Auxietre J-L, Meress F, Chamot-Rooke N. The final rifting evolution in the South China Sea. *Marine and Petroleum Geology*, 2014; 58: 704–720. doi: 10.1016/j.marpetgeo.2013.11.020.
- [3] Vijayan VR, Foss C, and Stagg H. Crustal character and thickness over the Dangerous Grounds and beneath the Northwest Borneo Trough. *Journal of Asian Earth Sciences*, 2013; 76: 389–398. doi: 10.1016/j.jseaes.2013.06.004.
- [4] Steuer S, Franke D, Meresse F, Savva D, Pubellier M, and Auxietre J-L. Oligocene-Miocene carbonates and their role for constraining the rifting and collision history of the Dangerous Grounds, South China Sea. *Marine and Petroleum Geology*, 2014; 58: 644–657. doi: 10.1016/j.marpetgeo.2013.12.010.

- [5] Chang JH, Hsu H-H, Liu Ch-S, Lee T-Y, Chiu S-D, Su Ch-Ch, Ma Y-F, Chiu Y-H, Hung H-T, Lin Y-Ch, Chiu Ch-H. Seismic sequence stratigraphic analysis of the carbonate platform, north offshore Taiping Island, Dangerous Grounds, South China Sea. *Tectonophysics*, 2017; 702:70–81. doi: 10.1016/j.tecto.2015.12.010.
- [6] Epting M. Sedimentology of Miocene carbonate build-ups, Central Luconia, offshore Sarawak. *Bulletin of Geological Society of Malaysia*, 1980; 12:17–30. doi:10.7186/bgsm12198002
- [7] Madon M. The Sabah Basin: Petroleum Geology and Resources of Malaysia. PETRONAS Internal book, 1999.
- [8] Yubo M, Shiguo W, Fuliang L, Dongdong D, Qiliang S, Yintao L, Mingfeng G. Seismic characteristics and development of the Xisha carbonate platforms, northern margin of the South China Sea. *Journal of Asian Earth Sciences*, 2011; 40(3): 770–783. doi: 10.1016/j.jseaes.2010.11.003.
- [9] Shao L, Cui Y, Qiao P, Zhang D, Liu X, and Zhang C. Sea-level changes and carbonate platform evolution of the Xisha Islands (South China Sea) since the Early Miocene. *Palaeogeography, Palaeoclimatology, Palaeoecology*, 2017; 485:504–516. doi: 10.1016/j.palaeo.2017.07.006.
- [10] Wilson MEJ. Cenozoic carbonates in Southeast Asia: Implications for equatorial carbonate development. *Sedimentary Geology*, 2002; 147(3–4): 295–428. doi: 10.1016/S0037-0738(01)00228-7.
- [11] Sun SQ and Esteban M. Paleoclimatic controls on sedimentation, diagenesis, and reservoir quality: lessons from Miocene carbonates. *American Association of Petroleum Geologists Bulletin*, 1994; 78(4):519–543. doi: 10.1306/bdff924e-1718-11d7-8645000102c1865d.
- [12] Ghosh DP. Seismic Attributes-Part-2, Methodology: E&P Application. CSI Internal book, 2016.
- [13] Hutchison CS, and Vijayan VR. What are the Spratly Islands? *Journal of Asian Earth Sciences*, 2010; 39(5):371–385. doi: 10.1016/j.jseaes.2010.04.013.
- [14] Banerjee A and Salim AMA. Seismic attribute analysis of deep-water Dangerous Grounds in the South China Sea, NW Sabah Platform region, Malaysia. *Journal of Natural Gas Science and Engineering*, 2020; 83: 103534. doi: 10.1016/j.jngse.2020.103534.
- [15] Kingston DR, Dishroon CP, and Williams PA. Global basin classification system. *American Association of Petroleum Geologist Bulletin (United States)*, 1983; 67:12.
- [16] Levell BK. The nature and significance of regional unconformities in the hydrocarbon-bearing Neogene sequence offshore West Sabah, 1987.
- [17] Milsom J, Holt R, bin Ayub D, and Smail R. Gravity anomalies and deep structural controls at the Sabah-Palawan margin, South China Sea. *Geological Society Special Publication London*, 1997; 126(126):417–427. doi: 10.1144/GSL.SP.1997.126.01.25.
- [18] Madon M, Kim CL, and Wong R. The structure and stratigraphy of deepwater Sarawak, Malaysia: Implications for tectonic evolution. *Journal of Asian Earth Sciences*, 2013; 76:312–333. doi: 10.1016/j.jseaes.2013.04.040.
- [19] Jong J, Nuraini DA, and Khamis MA. Basin modeling study of deepwater block R (DWR) offshore Sabah and its correlation with surface geochemical analyses. *Society of Petroleum Engineers - International Petroleum Technology Conference, Innovation and Collaboration: Keys to Affordable Energy*, 2014; 5: 3986–3996. doi: 10.2523/iptc-18186-ms.
- [20] Hinz K, and Schlüter HU. Geology of the Dangerous Grounds, South China Sea, and the Continental Margin off Southwest Palawan: Results of SONNE cruises SO-23 and SO-27. *Energy*, 1985; 10(3–4):297–315. doi: 10.1016/0360-5442(85)90048-9.
- [21] Kudrass HR, Wiedicke M, Cepek P, Kreuzer H, and Müller P. Mesozoic and Cainozoic rocks dredged from the South China Sea (Reed Bank area) and Sulu Sea and their significance for plate-tectonic reconstructions. *Marine and Petroleum Geology*, 1986; 3(1):19–30. doi: 10.1016/0264-8172(86)90053-X.
- [22] Peng X, Shen C, Mei L, Zhao Z, and Xie X. Rift–drift transition in the Dangerous Grounds, South China Sea. *Marine Geophysical Research*, 2019; 40(2):163–183. doi: 10.1007/s11001-018-9353-8.

- [23] Banerjee A, and Salim AMA. Stratigraphic evolution of deep-water Dangerous Grounds in the South China Sea, NW Sabah Platform Region, Malaysia. *Journal of Petroleum Science and Engineering*,2021;201:108434.  
[doi: 10.1016/j.petrol.2021.108434](https://doi.org/10.1016/j.petrol.2021.108434).
- [24] Banerjee A, Ghosh DP, Salim AMA, and Zakaria AA. Sub-surface investigation in the frontier region of deep-water NW Sabah, Malaysia. *APGCE*, 2019;1-5.  
[doi:10.3997/2214-4609.201903353](https://doi.org/10.3997/2214-4609.201903353)
- [25] Bitrus PR, Iacopini D, and Bond CE. Defining the 3D geometry of thin shale units in the Sleipner reservoir using seismic attributes. *Marine and Petroleum Geology*, 2016; 78: 405–425.  
[doi: 10.1016/j.marpetgeo.2016.09.020](https://doi.org/10.1016/j.marpetgeo.2016.09.020).
- [26] Zeng H. Stratal Slicing Makes Seismic Imaging of Depositional Systems Easier,2006; 40196.
- [27] Powers J Halliburton and Geomechanics International Announce strategic partnership. Press Release of Halliburton, Dallas, TX, USA,2000.
- [28] Bianco LCB and Halleck PM. Mechanisms of arch instability and sand production in two-phase saturated poorly consolidated sandstones. *The SPE European Formation Damage Conference:Hague,Netherlands:SPE-68932-MS*,2001.  
[doi.org/10.2118/68932-MS](https://doi.org/10.2118/68932-MS)
- [29] Acevedo S, Ranaudo MA, Escobar G, Gutiérrez L, Ortega P. Adsorption of asphaltenes and resins on organic and inorganic substrates and their correlation with precipitation problems in production well tubing. *Fuel*, 1995; 74: 595-598.
- [30] Bello R, and Onifade YS. Discrimination of reservoir fluid contacts using compressional and shear wave velocity. *Global Journal of Pure and Applied Sciences*,2016;22(2):177.  
[doi: 10.4314/gjpas.v22i2.7](https://doi.org/10.4314/gjpas.v22i2.7).
- [31] Buriyanyk M. Amplitude-vs-Offset and Seismic Rock Property Analysis: A Primer- CSEG RE-CORDER.The Canadian Society of Exploration Geophysicist Recorder, 2000.  
<https://csegrecorder.com/articles/view/amplitude-vs-offset-and-seismic-rock-property-analysis>.
- [32] Omudu L, and Ebeniro J. Cross-plotting of rock properties for fluid discrimination using well data in offshore Niger Delta. *Nigerian Journal of Physics*, 2006; 17(1):16–20.  
[doi: 10.4314/njphy.v17i1.37986](https://doi.org/10.4314/njphy.v17i1.37986).
- [33] Bello R, Igwenagu CL, Onifade Y. Cross plotting of Rock Properties for Fluid and Lithology Discrimination using Well Data in a Niger Delta Oil Field. *Journal of Applied Science and Environment*,2015;19(3).  
[doi.org/10.4314/jasem.v19i3.252015](https://doi.org/10.4314/jasem.v19i3.252015).
- [34] Burgess PM, Winefield P, Minzoni M, Elders C. Methods for identification of isolated carbonate build-ups from seismic reflection data. *American Association of Petroleum Geologists Bulletin*,2013;97:1071-1098.  
[doi.org/10.1306/12051212011](https://doi.org/10.1306/12051212011).
- [35] Vincentelli MGC, Contreras SAC, Chaves MU. Geophysical characterization of Albian carbonates reservoirs in Brazilian basins: The sweetness as a tool for carbonate reservoirs definition. *Brazilian Journal of Geophysics*,2014;32:695-705.  
[doi.org/10.22564/rbgf.v32i4.538](https://doi.org/10.22564/rbgf.v32i4.538)
- [36] Yuliandri I, Usman T, Panguriseng M. Seismic based characterization of Baturaja Carbonate at 3D Topaz Area,2012. Adapt from Ext. Abstr. Prep. conjunction with poster Present. AAPG Int. Conv. Exhib. Milan, Italy, 2011;50531.
- [37] Ødegaard E, Avseth P. Well log and seismic data analysis using rock physics templates. *First Break*,2004;22:37-43.  
[doi.org/10.3997/1365-2397.2004017](https://doi.org/10.3997/1365-2397.2004017)
- [38] Wu S, Yang Z, Wang D, Lü F, Lüdmann T, Fulthorpe C, and Wang B. Architecture, development and geological control of the Xisha carbonate platforms, northwestern South China Sea. *Marine Geology*,2014; 350: 71-83.  
[doi.org/10.1016/j.margeo.2013.12.016](https://doi.org/10.1016/j.margeo.2013.12.016)
- [39] Vahrenkamp VC. Miocene carbonates of the Luconia province, offshore Sarawak: implications for regional geology and reservoir properties from Strontium-isotope stratigraphy. *Geological Society of Malaysia Bulletin*,1998;42:1-13.  
[doi.org/10.7186/bgsm42199801](https://doi.org/10.7186/bgsm42199801)
- [40] Hutchison CS. The North-West Borneo Trough. *Marine Geology*,2010;271:32-43.  
[doi.org/10.1016/j.margeo.2010.01.007](https://doi.org/10.1016/j.margeo.2010.01.007)



- [41] Li L, Clift PD, Stephenson R, Nguyen HT. Non-uniform hyper-extension in advance of seafloor spreading on the Vietnam continental margin and the SW South China Sea. *Basin Research*,2014;26:106-134.  
[doi.org/10.1111/bre.12045](https://doi.org/10.1111/bre.12045)
- [42] Briaies A, Patriat P, Tapponnier P. Updated interpretation of magnetic anomalies and seafloor spreading stages in the south China Sea: Implications for the Tertiary tectonics of Southeast Asia. *Journal of Geophysical Research: Solid Earth*,1993;98:6299-6328.  
[doi.org/10.1029/92jb02280](https://doi.org/10.1029/92jb02280)
- [43] Haq BU, Hardenbol J, Vail PR. Mesozoic and Cenozoic chronostratigraphy and cycles of sea-level change. In book *Sea-Level Changes: An Integrated Approach* Edition: SEPM Special Publication 42 Publisher: SEPM, Tulsa, Oklahoma, USA. Editors: C. K. Wilgus, B. S. Hastings, C. G. St. C. Kendall, C. A. Ross, J. C. Van Wagoner, 1988.  
[doi.org/10.2110/pec.88.01.0071](https://doi.org/10.2110/pec.88.01.0071)
- [44] Ogg JG, Ogg GM, Gradstein FM. A concise geologic time scale. eBook ISBN: 9780444594686, 2016.
- [45] Clift P, Lee GH, Duc NA, Barckhausen U, van Long H, and Zhen S. Seismic reflection evidence for a Dangerous Grounds miniplate: No extrusion origin for the South China Sea. *Tectonics*,2008;27:1-16.  
[doi.org/10.1029/2007TC002216](https://doi.org/10.1029/2007TC002216)
- [46] Ding W, Franke D, Li J, Steuer S. Seismic stratigraphy and tectonic structure from a composite multi-channel seismic profile across the entire Dangerous Grounds, South China Sea. *Tectonophysics*, 2013; 582:162–176.  
[doi.org/10.1016/j.tecto.2012.09.026](https://doi.org/10.1016/j.tecto.2012.09.026)

---

*To whom correspondence should be addressed: Dr. Atanu Banerjee, Centre for Subsurface Imaging, Department of Geosciences, Universiti Teknologi PETRONAS, 32610, Seri Iskandar, Perak, Malaysia,  
E-mail: [atanu.ism@gmail.com](mailto:atanu.ism@gmail.com)*